

Article

# Conventional and Second Order Sliding Mode Control of Permanent Magnet Synchronous Motor Fed by Direct Matrix Converter: Comparative Study †

Abdelhakim Dendouga 

LI3CUB-Research Lab., Department of Electrical Engineering, University of Biskra, 07000 Biskra, Algeria; a.dendouga@univ-biskra.dz; Tel.: +213-6-7400-6720

† This Paper Is an Extended Version of Our Paper Published in 20th IEEE International Conference on Environment and Electrical Engineering (EEEIC 2020), Web Conference, Madrid, Spain, 9–12 June 2020, pp. 1867–1871.

Received: 25 August 2020; Accepted: 25 September 2020; Published: 30 September 2020



**Abstract:** The main objective of this work revolves around the design of second order sliding mode controllers (SOSMC) based on the super twisting algorithm (STA) for asynchronous permanent magnet motor (PMSM) fed by a direct matrix converter (DMC), in order to improve the effectiveness of the considered drive system. The SOSMC was selected to minimize the chattering phenomenon caused by the conventional sliding mode controller (SMC), as well to decrease the level of total harmonic distortion (THD) produced by the drive system. In addition, the literature has taken a great interest in the STA due to its robustness to modeling errors and to external disturbances. Furthermore, due to its low conduction losses, the space vector approach was designated as a switching law to control the DMC. In addition, the topology and design method of the damped passive filter, which allows improvement of the waveform and attenuation of the harmonics of the input current, have been detailed. Finally, to discover the strengths and weaknesses of the proposed control approach based on SOSMC, a comparative study between the latter and that using the conventional SMC was executed. The results obtained confirm the effectiveness of SOSMC over the conventional SMC under different operating conditions.

**Keywords:** permanent magnet synchronous motor; direct matrix converter; space vector modulation; damped passive filter; conventional sliding mode controller; second order sliding mode controller; stator current orientation control

## 1. Introduction

The direct matrix converter (DMC) is an AC–AC converter that converts electrical energy directly without any intermediate element, by the connection of each phase of the load by any one of three phases in the grid side for each time, according to a suitable switching algorithm [1–3]. The DMC requires fully controlled bidirectional switches, which allow operation in four-quadrants, bidirectional power flow, and adjustable power factor (Figure 1) [4,5]. According to the literature, space vector modulation (SVM) is the most popular approach for many researchers to control the DMC, since it exhibits low conduction losses [1,6]. To improve the input current waveform, to therefore reduce the harmonic distortion rate, the DMC must be connected to the grid via a passive filter. There are various topologies that have been proposed in research works [1,2,7–10]; however, the passive filter with a damping resistor connected in parallel with the inductor has been strongly recommended for DMC [7,8]. Due to its many previously mentioned advantages, it is estimated that the DMC will become the most popular candidate in the variable speed field, especially in drive and generation systems.

Recently, due to its exceptional advantages—high efficiency and power density, low inertia, operating with a power factor unit, and excellent reliability with low maintenance cost—the permanent magnet synchronous machine (PMSM) has become the most suitable candidate in the academic and industrial sector, for drive and generation applications, especially in the systems where quick torque response without any overshoot is required [11–13]. Conventionally, the PMSM is supplied by a back to back converter. Actually, thanks to the development of microelectronics and computer technology, the DMC is becoming the most suitable converter for PMSM, with regard to the excellent performances it provides [1,9,14,15].

Several approaches have been suggested in the literature to control the PMSM. However, it can be mentioned that vector orientation control (VOC) and direct torque control (DTC) are the most used techniques, up to the present time, due to their satisfactory performance [1,9,11,14–16]. Exceptionally, other control methods based on the predictive model and on feedback linearization have been introduced in the work [17–19]. However, the advantages provided by these methods are not sufficiently significant if taking into account their complexities to implement. Concerning DTC control, the issue of high torque ripple in low speed operation was the major obstacle of this method [14]. Therefore, VOC still remains one of the most preferred techniques, especially with regard to its high performance as well as its simplicity and ease of implementation. However, the use of PI controllers leads to a degradation of the performance of the VOC, with respect to the variation of parameters and operation at high speeds [1,2]. Thus, the use of robust controllers is highly recommended to improve the performance of VOC. According to the literature, it is found that the sliding mode controllers (SMCs) exhibit a very high effectiveness with regard to decoupling, robustness, and insensitivity to parameter variations and external disturbances [1,14,15].

Despite the high performance provided by the conventional so-called first-order SMCs, the presence of the chattering phenomenon (high frequency oscillations due to controller switching) is a major drawback for this type of controller [12,20–22]. To overcome this problem, the second order sliding mode controller (SOSMC) based on the super-twisting algorithm (STA) has been strongly suggested as a solution to reduce the impact of chattering. Since, the STA has proven its robustness in terms of precision against the errors of modeling and the disturbances [12,21].

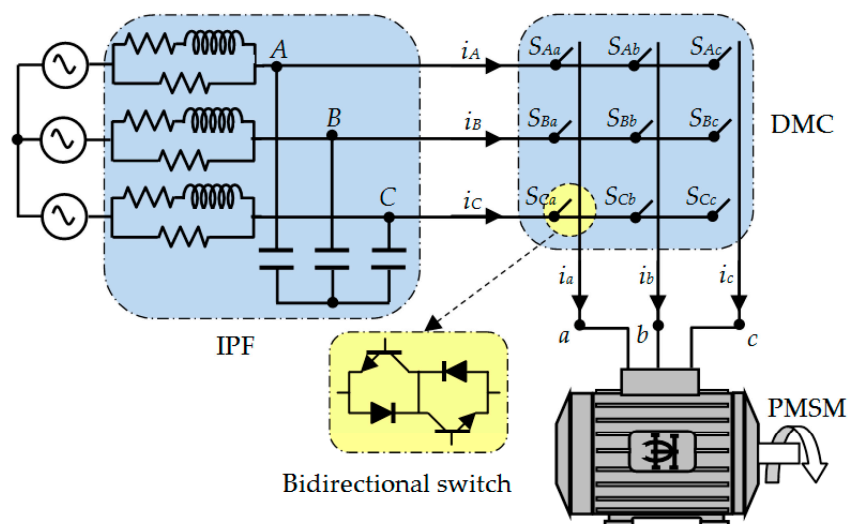


Figure 1. Descriptive diagram of DMC fed PMSM drive system.

The objective of this work is focused on the design of SOSMCs based on the STA for the vector control of PMSM fed by the DMC, in order to improve the effectiveness and robustness of the considered drive system. In this context, the SOSMC was selected to minimize the chattering phenomenon caused by the conventional SMC, as well to decrease the level of total harmonic distortion (THD). A simple method was chosen among several existing in the literature to design the SOSMC based on STA in an

easy way. The vector control was implemented taking into account the orientation of the stator current along the d axis of the synchronous reference frame fixed to the rotor. On the other side, the SVM strategy has also been implemented to control the DMC due to its success with regard to its reduced conduction losses. In addition, the topology and design method of the damped passive filter, which allows the improvement of the waveform and the attenuation of the harmonics of the input current, have been well detailed. Finally, to discover the strengths and weaknesses of the proposed control approach based on SOSMC, a comparative study between the latter and that using the conventional SMC was executed.

## 2. Modeling and Control Strategy

### 2.1. Modeling of PMSM

Assuming that the operating conditions are balanced, the distribution of windings is symmetrical, the magnetic circuits are linear, and the magnetic field is sinusoidal in the air gap, the PMSM can be represented in the synchronous reference related to the rotor, as shown by Figure 2 [1,16].

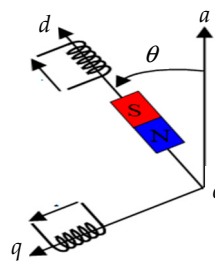


Figure 2. Two-phase representation of PMSM.

The stator voltage equations are given by

$$\begin{cases} v_d = R_s i_d + \frac{d\varphi_d}{dt} - \omega_{syn} \varphi_q, \\ v_q = R_s i_q + \frac{d\varphi_q}{dt} + \omega_{syn} \varphi_d, \end{cases} \quad (1)$$

where  $\varphi_d = L_d i_d + \varphi_{pf}$ ,  $\varphi_q = L_q i_q$ ,  $\omega_{syn} = n_p \omega_m$ .

The development of Equation (1) allows for the writing of

$$\begin{cases} \frac{di_d}{dt} = -\frac{R_s}{L_d} i_d + \omega_{syn} \frac{L_q}{L_d} i_q + \frac{1}{L_d} v_d, \\ \frac{di_q}{dt} = -\frac{R_s}{L_d} i_q - \frac{\omega_{syn}}{L_q} (L_d i_d + \varphi_{pf}) + \frac{1}{L_q} v_q, \\ \frac{d\omega_m}{dt} = \frac{1}{J} (T_e - T_L - B\omega_m), \end{cases} \quad (2)$$

The electromechanical torque is determined by

$$T_e = \frac{3}{2} n_p [(L_d - L_q) i_d i_q + \varphi_{pf} i_q], \quad (3)$$

$v_d, v_q, i_d, i_q, \varphi_d, \varphi_q$ :  $d$ - $q$  components of stator voltages, currents, and flux;

$\varphi_{pf}$ : the permanent rotor flux;

$R_s, L_d, L_q$ : the resistance, and direct and quadratic inductances of the stator;

$T_L, \omega_{syn}, \omega_m, n_p$ : the load torque, synchronous and rotor speeds, and the number of pole pairs;

$J, B$ : the rotor inertia and the viscous friction coefficient.

## 2.2. Stator Current Orientation Control

The objective of this strategy is to control the PMSM in a way that achieves a behavior similar to that of the DC motor. For that, the current vector of the stator must coincide with the axis  $q$ ; therefore, its component  $d$  is zero [1,14]. In this condition, Equation (3) can be reduced as

$$T_e = \frac{3}{2} n_p \varphi_{pf} i_{qref}, \quad (4)$$

From (2), assuming that

$$\begin{cases} v_d = v_{d1} - e_d, \\ v_q = v_{q1} + e_q, \end{cases} \quad (5)$$

where

$$\begin{cases} v_{d1} = R_s i_d + L_d \frac{di_d}{dt}, \\ v_{q1} = R_s i_q + L_q \frac{di_q}{dt}, \end{cases} \quad (6)$$

and

$$\begin{cases} e_d = L_q \omega_{syn} i_q, \\ e_q = \omega_{syn} (L_d i_d + \varphi_{pf}), \end{cases} \quad (7)$$

$e_d$  and  $e_q$  are the terms that must be compensated to have a decoupled control of  $i_d$  and  $i_q$ .

## 2.3. Design of Conventional Sliding Mode Controllers (SMC)

To ensure good tracking, timely and accurate response, and insensitivity to changes in drive system parameters, three sliding mode controllers have been designed to control the speed and both components of the stator current.

### 2.3.1. For the Speed

For the speed, the sliding surface is chosen as

$$S_\omega = \omega_{mref} - \omega_m, \quad (8)$$

The derivative of (8) is deduced by considering (2) and (4)

$$\dot{S}_\omega = \dot{\omega}_{mref} - \frac{1}{J} \left( \frac{3}{2} n_p \varphi_{pf} i_{qref} - T_L - B\omega_m \right), \quad (9)$$

The reference control variable is expressed as follows:

$$i_{qref} = i_{qeq} + i_{qn}, \quad (10)$$

$i_{qeq}$  and  $i_{qn}$  are the equivalent and switching components of the control variable, respectively.

The equivalent component is deduced in the mode of sliding mode ( $\dot{S}_\omega = 0$ ) [1,2,23], which gives

$$i_{qeq} = \frac{2}{3} \left( \frac{J \dot{\omega}_{mref} + T_L + B\omega_m}{n_p \varphi_{pf}} \right), \quad (11)$$

The switching component of the controller is expressed by

$$i_{qn} = K_\omega \text{sign}(S_\omega), \quad (12)$$

To guarantee the convergence condition, the Lyapunov equation must be verified [1,23]

$$\dot{V} = S_\omega \dot{S}_\omega < 0, \quad (13)$$

By replacing (12) and (11) in (10), and then in (9), which allows the writing of

$$\dot{S}_\omega = -\frac{3}{2J} n_p \varphi_{pf} K_\omega \text{sign}(S_\omega), \quad (14)$$

Consequently, the condition (12) is verified when

$$\begin{cases} \text{if } \text{sign}(S_\omega) > 0 \Rightarrow \dot{S}_\omega < 0, \\ \text{if } \text{sign}(S_\omega) < 0 \Rightarrow \dot{S}_\omega > 0, \end{cases} \quad (15)$$

Thus,  $K_\omega$  is a positive constant.

### 2.3.2. For the $i_d$ and $i_q$

The  $i_d$  and  $i_q$  current controllers are designed with the same procedure as that of the speed controller. The sliding mode surfaces are defined by

$$\begin{cases} S_d = i_{dref} - i_d, \\ S_q = i_{qref} - i_q, \end{cases} \quad (16)$$

The derivative of (16) is

$$\begin{cases} \dot{S}_d = \dot{i}_{dref} - \dot{i}_d, \\ \dot{S}_q = \dot{i}_{qref} - \dot{i}_q, \end{cases} \quad (17)$$

The reference voltages are given by

$$\begin{cases} v_{d1ref} = v_{deq} + v_{dn}, \\ v_{1qref} = v_{qeq} + v_{qn}, \end{cases} \quad (18)$$

Taking into account the condition of the sliding mode, the equivalent components of voltage can be deduced from Equations (17) and (2), as following

$$\begin{cases} v_{deq} = L_d \dot{i}_{dref} + R_s i_d - \omega_{syn} L_q i_q, \\ v_{qeq} = L_q \dot{i}_{qref} + R_s i_q + \omega_{syn} L_d i_d + \omega_s \varphi_{pf}, \end{cases} \quad (19)$$

The switching components have as expressions

$$\begin{cases} v_{dn} = K_d \text{sign}(S_d), \\ v_{qn} = K_q \text{sign}(S_q), \end{cases} \quad (20)$$

Considering the Lyapunov condition,  $K_d$  and  $K_q$  are positive constants.

### 2.4. Design of Second Order Sliding Mode Controllers (SOSMC)

The equivalent components of  $i_{qref}$ ,  $v_{dref}$  and  $v_{qref}$  are the same obtained by Equations (11) and (19). Only the expressions of the switching components will change.

#### 2.4.1. For the Speed

The second derivative of (9) has the form [12,20,24]

$$\ddot{S}_\omega = \psi(t, x) + \zeta(t, x)\dot{i}_{qref}, \quad (21)$$

$$|\psi| \leq \Phi, \Phi > 0, 0 < \Gamma_m \leq \zeta \leq \Gamma_M.$$

$\psi(t, x)$  and  $\zeta(t, x)$  are uncertain functions.

According to the STA, the switching component of  $i_{qref}$  is defined as [21,23,24]

$$i_{qn} = k_{\omega 1}|S_\omega|^{1/2}\text{sign}(S_\omega) + k_{\omega 2} \int \text{sign}(S_\omega)dt, \quad (22)$$

Considering the Lyapunov condition (13),  $K_d$  and  $K_q$  are positive constants.

The conditions of convergence in finite time to the sliding manifold are guaranteed if [12,20]

$$\begin{cases} k_{\omega 2} > \frac{\Phi}{\Gamma_m}, \\ k_{\omega 1}^2 \geq \frac{4\Phi}{\Gamma_m^2} \frac{\Gamma_M(W+\Phi)}{\Gamma_m(W-\Phi)}, \end{cases} \quad (23)$$

In the literature, there exists a simple formula which was proposed by [21,25], which also ensures the convergence conditions ( $S_\omega = \dot{S}_\omega = 0$ ), if the input signal is a measurable locally bounded function, and it has a derivative with Lipschitz's constant  $C_\omega > 0$ .

This formula is given by

$$\begin{cases} k_{\omega 2} > C_\omega, \\ k_{\omega 1}^2 \geq 4C_\omega \frac{k_{\omega 2} + C_\omega}{k_{\omega 2} - C_\omega}, \end{cases} \quad (24)$$

In addition, the expression (24) can be approximated to [21,23,25]

$$\begin{cases} k_{\omega 1} = 1.5 \sqrt{C_\omega}, \\ k_{\omega 2} = 1.1C_\omega, \end{cases} \quad (25)$$

The approach given by expression (25) makes it possible to obtain rapid convergence and high accuracy. However, it should be noted that this approach is valid only for bounded disturbances, which require a conservative upper limit when designing the controller to maintain the sliding mode regime [21,23].

#### 2.4.2. For the $i_d$ and $i_q$

The  $i_d$  and  $i_q$  current controllers are designed with the same procedure as that of the speed controller.

The switching components are defined by

$$\begin{cases} v_{dn} = k_{d1}|S_d|^{1/2}\text{sign}(S_d) + k_{d2} \int \text{sign}(S_d)dt, \\ v_{qn} = k_{q1}|S_q|^{1/2}\text{sign}(S_q) + k_{q2} \int \text{sign}(S_q)dt, \end{cases} \quad (26)$$

where

$$\begin{cases} k_{d1} = 1.5 \sqrt{C_d}, \\ k_{d2} = 1.1C_d, \end{cases} \quad (27)$$

and

$$\begin{cases} k_{q1} = 1.5 \sqrt{C_q}, \\ k_{q2} = 1.1C_q, \end{cases} \quad (28)$$

To limit overshoot of the speed response, a low pass filter can be inserted for the reference speed [1,2].

$$F_\omega = \frac{1}{1 + \tau_f s'} \tag{29}$$

### 3. SVM Switching Algorithm for DMC

Considering that the voltage sources must not be in short circuit and the current sources must not be in open circuit, amongst the 27 possible configurations for DMC, just 21 possible switching states indicated by 18 vectors stationary ( $\pm 1, \pm 2, \pm 3, \pm 4, \pm 5, \pm 6, \pm 7, \pm 8, \pm 9$ ) and 3 null vectors ( $0_a, 0_b, 0_c$ ), are exploited by the SVM switching algorithm to generate the preferred output voltage vector  $v_o$  and the input current vector  $i_i$  for the DMC (See Table 1) [1,2,7]. The projection of the stationary vectors for the output voltage and input current in the plane ( $\alpha, \beta$ ) enables the shaping of two regular hexagons of six sectors each, so that the sector is bounded by two consequential vectors (Figure 3).

Table 1. Switching configurations.

Switching Configuration	Switches On	Switching Configuration	Switches On
+1	$S_{aA}S_{bB}S_{cC}$	-1	$S_{bA}S_{aB}S_{aC}$
+2	$S_{bA}S_{cB}S_{cC}$	-2	$S_{cA}S_{bB}S_{bC}$
+3	$S_{cA}S_{aB}S_{aC}$	-3	$S_{aA}S_{cB}S_{cC}$
+4	$S_{bA}S_{aB}S_{bC}$	-4	$S_{aA}S_{bB}S_{aC}$
+5	$S_{cA}S_{bB}S_{cC}$	-5	$S_{bA}S_{cB}S_{bC}$
+6	$S_{aA}S_{cB}S_{aC}$	-6	$S_{cA}S_{aB}S_{cC}$
+7	$S_{bA}S_{bB}S_{aC}$	-7	$S_{aA}S_{aB}S_{bC}$
+8	$S_{cA}S_{cB}S_{bC}$	-8	$S_{bA}S_{bB}S_{cC}$
+9	$S_{aA}S_{aB}S_{cC}$	-9	$S_{cA}S_{cB}S_{aC}$
$0_a$	$S_{aA}S_{aB}S_{aC}$	$0_b$	$S_{bA}S_{bB}S_{bC}$
$0_c$	$S_{cA}S_{cB}S_{cC}$		

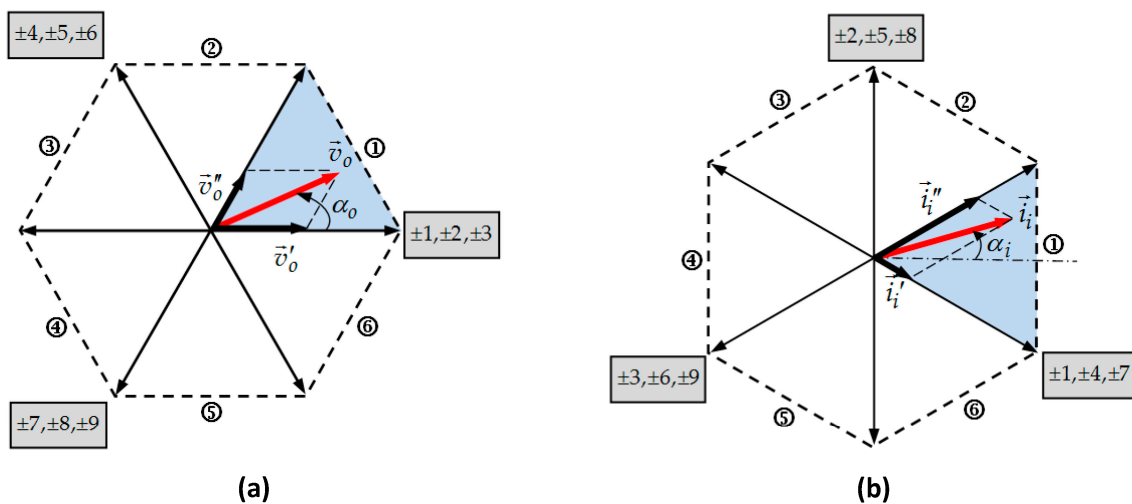


Figure 3. Vector hexagons formed by (a)  $\vec{v}_o$  and (b)  $\vec{i}_i$ .

According to the position of two vectors  $v_o$  and  $i_i$  in the two hexagons, the SVM algorithm consists of selecting four stationary vectors which are applied for each modulation period to calculate the

switching times (Table 2). In addition, the null vectors are also used to complete the modulation period. The switching times are calculated by the following equations [1,2]:

$$\begin{cases} \delta_1 = \frac{2}{\sqrt{3}}q_v \sin\left[\alpha_o - (k_v - 1)\frac{\pi}{3}\right] \sin\left[\frac{\pi}{6} - \left(\alpha_i - (k_i - 1)\frac{\pi}{3}\right)\right], \\ \delta_2 = \frac{2}{\sqrt{3}}q_v \sin\left[\alpha_o - (k_v - 1)\frac{\pi}{3}\right] \sin\left[\frac{\pi}{6} + \left(\alpha_i - (k_i - 1)\frac{\pi}{3}\right)\right], \\ \delta_3 = \frac{2}{\sqrt{3}}q_v \sin\left[k_v\frac{\pi}{3} - \alpha_o\right] \sin\left[\frac{\pi}{6} - \left(\alpha_i - (k_i - 1)\frac{\pi}{3}\right)\right], \\ \delta_4 = \frac{2}{\sqrt{3}}q_v \sin\left[k_v\frac{\pi}{3} - \alpha_o\right] \sin\left[\frac{\pi}{6} + \left(\alpha_i - (k_i - 1)\frac{\pi}{3}\right)\right], \\ \delta_0 = 1 - (\delta_1 + \delta_2 + \delta_3 + \delta_4), \end{cases} \quad (30)$$

$q_v = V_o/V_i$  is ratio of voltage;

$\alpha_o, \alpha_i, k_v,$  and  $k_i$  are the phase angles and the sector number of  $\vec{v}_o$  and  $\vec{i}_i$ , respectively.

**Table 2.** Stationary vectors selected by SVM for each  $\vec{v}_o$  and  $\vec{i}_i$  sectors.

		Sector Number of $\vec{v}_o$					
		1	2	3	4	5	6
Switching Times		$\delta_1\delta_2\delta_3\delta_4$	$\delta_1\delta_2\delta_3\delta_4$	$\delta_1\delta_2\delta_3\delta_4$	$\delta_1\delta_2\delta_3\delta_4$	$\delta_1\delta_2\delta_3\delta_4$	$\delta_1\delta_2\delta_3\delta_4$
	Sector number $i_i$						
1	1	-7 +9 +1 -3	+4 -6 -7 +9	-1 +3 +4 -6	+7 -9 -1 +3	-4 +6 +7 -9	+1 -3 -4 +6
	2	+9 -8 -3 +2	-6 +5 +9 -8	+3 -2 -6 +5	-9 +8 +3 -2	+6 -5 -9 +8	-3 +2 +6 -5
	3	-8 +7 +2 -1	+5 -4 -8 +7	-2 +1 +5 -4	+8 -7 -2 +1	-5 +4 +8 -7	+2 -1 -5 +4
	4	+7 -9 -1 +3	-4 +6 +7 -9	+1 -3 -4 +6	-7 +9 +1 -3	+4 -6 -7 +9	-1 +3 +4 -6
	5	-9 +8 +3 -2	+6 -5 -9 +8	-3 +2 +6 -5	+9 -8 -3 +2	-6 +5 +9 -8	+3 -2 -6 +5
	6	+8 -7 -2 +1	-5 +4 +8 -7	+2 -1 -5 +4	-8 +7 +2 -1	+5 -4 -8 +7	-2 +1 +5 -4

#### 4. Damped Passive Input Filter

To improve the input current waveform, to therefore reduce the harmonic distortion rate, the DMC must be connected to the grid via a passive filter.

In context, the passive filter with a damping resistor connected in parallel with the inductor illustrated by Figure 4 has been strongly recommended for this type of converter [7,8].

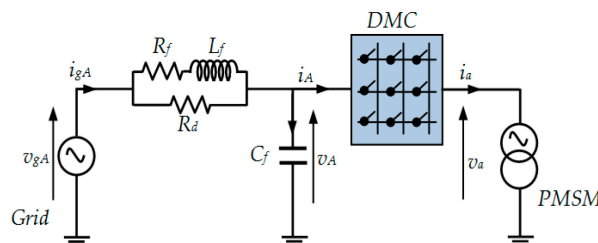


**Figure 4.** Single phase presentation of passive filter recommended for the DMC.

Its transfer function is given by the following expressions

$$V_A(s) = \frac{(L_f \cdot s + R_d + R_f) \cdot V_{gA}(s) - R_d \cdot (L_f \cdot s + R_f) \cdot I_A(s)}{R_d \cdot L_f \cdot C_f \cdot s^2 + (R_d \cdot R_f \cdot C_f + L_f) \cdot s + (R_d + R_f)}, \quad (31)$$

$$I_{gA}(s) = \frac{[L_f \cdot C_f \cdot s^2 + (R_d + R_f) \cdot C_f \cdot s] \cdot V_{gA}(s) + [L_f \cdot s + R_d + R_f] \cdot I_A(s)}{R_d \cdot L_f \cdot C_f \cdot s^2 + (R_d \cdot R_f \cdot C_f + L_f) \cdot s + (R_d + R_f)}, \quad (32)$$

The frequency  $\omega_n$  and damping factor  $\zeta$  of the denominator are expressed by

$$\begin{cases} \omega_n = \sqrt{\frac{R_d + R_f}{R_d L_f C_f}}, \\ \zeta = \frac{R_d R_f C_f + L_f}{2 \sqrt{R_d L_f C_f (R_d + R_f)}}, \end{cases} \quad (33)$$

Considering that:  $R_d \gg (R_d \rightarrow \infty)$  and  $R_f = \text{few ohms}$ . The expression (33) is simplified to

$$\begin{cases} \omega_n = \frac{1}{\sqrt{L_f C_f}}, \\ \zeta = \frac{1}{2R_d} \sqrt{\frac{L_f}{C_f}}, \end{cases} \quad (34)$$

## 5. Results and Discussions

The performance and effectiveness of the current orientation control of the DMC-fed PMSM drive system using the SOSMC based on the STA, compared to that using the conventional SMC, are examined through a simulation study, considering Figure 5. The parameters of the drive system are illustrated in Table 3 [12]. Under the same conditions, the different robustness tests listed below were applied for the two types of controllers:

- Startup mode (unloaded  $T_L = 0$ ), with a desired speed 100 rd/s (0–0.5 s);
- From 0.5 to 2 s, the motor is loaded by a load of 10 N m, and after 2 s, the motor is unloaded again;
- Parameters variation: Stator resistance from the value  $R_s$  to  $2R_s$  (at  $t = 1.5$  s) and rotor inertia from J to 2J (at  $t = 1$  s);
- Rotation direction reversing (2.5–3 s);
- Under-speed operation (3–3.5 s);
- Over-speed operation (3.5–4 s).

**Table 3.** Drive system parameters.

PMSM							
$P_n$	$R_s$	$L_d$	$L_q$	$\Phi_f$	$J$	$B$	$n_p$
1.5 kW	1.4 $\Omega$	0.0066 H	0.0058 H	0.1546 Wb	0.00176 kg m <sup>2</sup>	0.00038 Nm/rd	3
Passive Filter							
$R_d$	$R_f$	$L_f$	$C_f$				
30 $\Omega$	0.1 $\Omega$	0.1 H	47 $\mu$ F				
SOSMC							
$k_{\omega 1}$	$k_{\omega 2}$	$k_{d1}$	$k_{d2}$	$k_{q1}$	$k_{q2}$		
4.7434	11	33.5	550	23.7	275		
SMC							
$k_{\omega}$	$k_d$	$k_q$					
5	100	50					

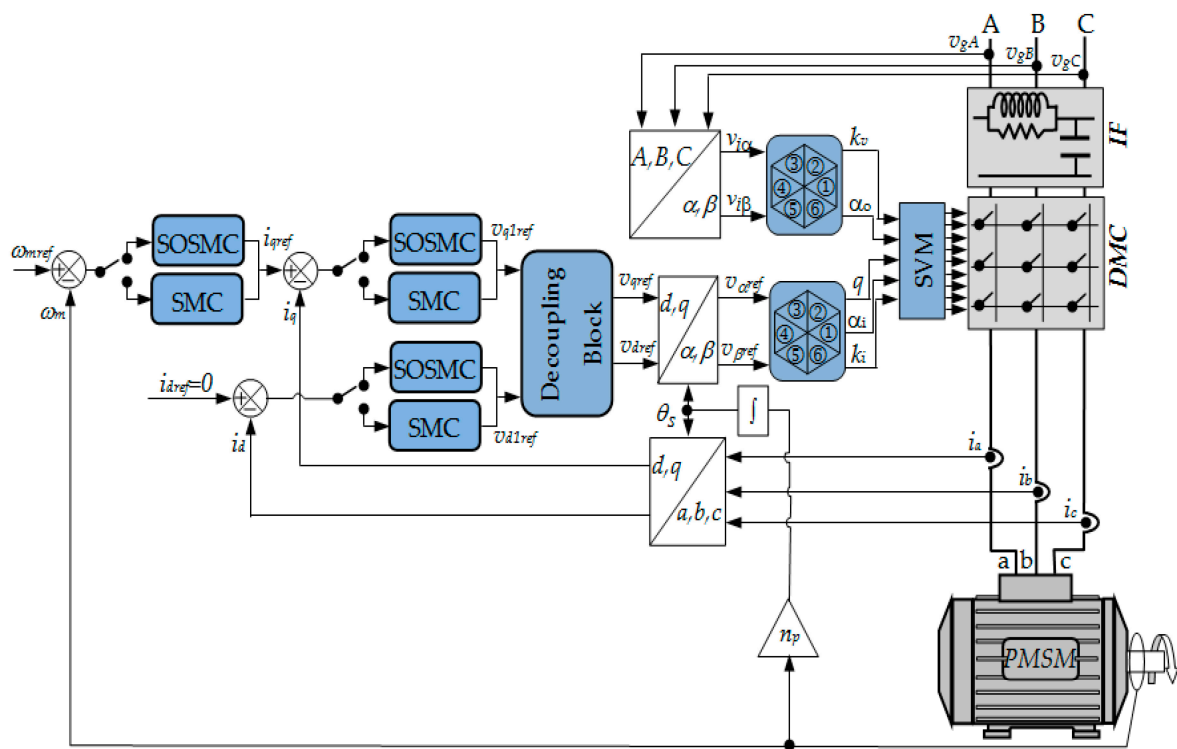


**Figure 5.** Synoptic scheme of current-orientation control of the DMC-fed PMSM drive system using the SOSMC based on the STA and conventional SMC.

From the results illustrated in Figure 6, it was clear that the proposed control law (stator current-orientation control) provided good robustness and high performance regarding the excellent reference tracking, rapid response, and the in sensitivity to change of parameters. As well, the small mechanical time constant obtained for the speed is reflected the low inertia which characterizes the PMSM. The comparison study between the two types of sliding mode controllers used by the considered method makes it possible to know the strengths and weaknesses of each type.

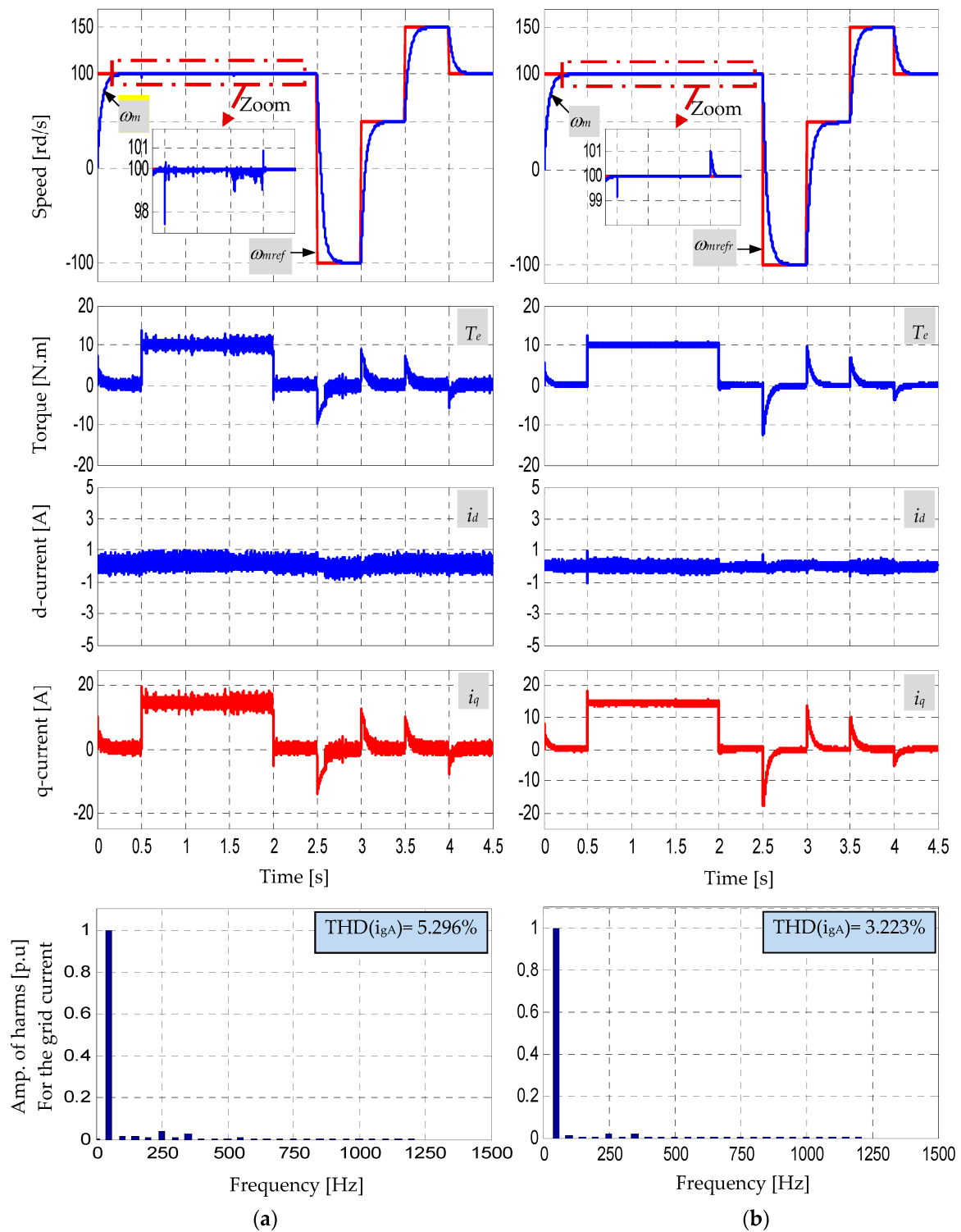


**Figure 6.** Simulation results of speed, electro-mechanical torque,  $d$ - $q$  components of stator current and harmonic spectrum of input current in the grid side for each controller: (a) SMC; (b) SOSMC.

The comparative analysis is summarized in the following points:

1. For the conventional SMC: from Figure 6a, it can be seen that the speed has a good tracking of its reference trajectory with a very short response time, with the exception of a negligible exceeding at the moment of application of the load torque (0.5–2 s). As can be seen, no influence was detected from the variation of the parameters (variation of  $R_s$  and  $J$  at  $t = 1.5$  s and  $t = 1$  s) on the

performance of the control. According to the  $i_d$  and  $i_q$  curves, it can be noted that a decoupled control has been maintained regardless of the operating mode of the drive system. However, the presence of chattering in the torque and current responses, as well as the high harmonic rate (THD = 5.296%; greater than 5%, it is not compliant to IEEE standard) constitute the weak points of the conventional SMC.

- For the SOSMC: from Figure 6b, the good tracking, rapid response, decoupling between  $i_d$  and  $i_q$ , and the insensitivity to parameters variation were also obtained by the SOSMC. Besides these advantages, this type of controller allows the attenuation of chattering, as well as it allows the obtaining of a low rate of harmonic distortion (THD = 3.223, compliant with IEEE standard). To present this study in a more comprehensive way, Table 4, which summarizes all the points mentioned above, has been used.

**Table 4.** Summary table for the comparison study.

Controller	Tracking	Response Time	Decoupled Control	Chattering Existence	THD
SMC	good	good	good	high	high (>5%)
SOSMC	good	good	good	low	low (<5%)

Therefore, the comparison analysis clearly confirms the effectiveness and high performance of SOSMC over the conventional SMC for the different robustness tests, in terms of chattering attenuation and the low rate of harmonic distortion. Consequently, the SOSMC based on the STA constitutes an interesting solution for the systems, which require a high accuracy of the pursuit to the imposed reference trajectory, with very low chattering. This idea does not preclude exploiting other approaches that exist in the literature to further mitigate chattering; for example, SOSMC with adaptive gains, SOSMC associated with fuzzy logic.

Figure 7 shows the waveforms obtained by using the SOSMC controller.

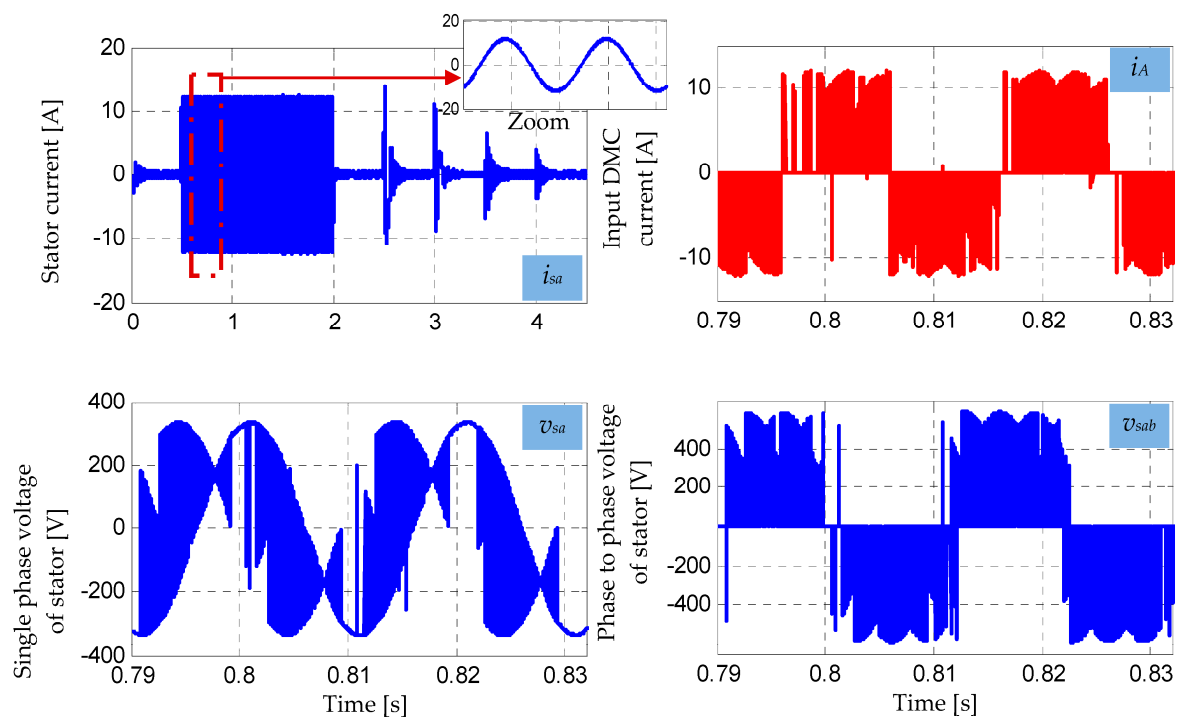


**Figure 7.** Waveforms of stator current, single and phase to phase voltage, and input current of DMC.

From Figure 7, one can see that the waveform of stator voltage ( $v_{sa}, v_{sab}$ ) is deduced from the input voltage and also the waveform of input current of the DMC ( $i_A$ ) is deduced from the output current of this later, by using a switching algorithm established by the SVM strategy. It can also be mentioned that the stator current ( $i_{sa}$ ) has a nearly sinusoidal form.

## 6. Conclusions

The results obtained by simulation study clearly show the excellent robustness and high performance of the proposed control law for the permanent magnet synchronous motor fed by the direct matrix converter (PMSM-DMC) drive system, regarding good reference tracking, rapid response, and in sensitivity to change of parameters. On the other hand, the comparative study undoubtedly confirms that the second order sliding mode controller (SOSMC) provides interesting improvements over the conventional sliding mode control (SMC) in terms of chattering attenuation and reduction of harmonic distortion rate.

The passive filter with a damping resistor connected in parallel with the inductor is strongly required for the direct matrix converter (DMC). In this work, a simple and easy design method is proposed to calculate the parameters of this filter. This method achieves an almost sinusoidal current waveform in the grid side, which also allows reduction in the rate of harmonic distortion.

The solution proposed in this work is appropriate for all high dynamic performance applications where good tracking without chattering, accuracy, and a low level of harmonic distortion are highly required.

As a prospect for future research, the encouraging results obtained will constitute a solid basis for an experimental implementation of the proposed drive system. As the matrix converter (MC) is not really available for all researchers, this work was verified by simulation.

**Funding:** This research was supported by the Algerian General Direction of Higher Education and Training (DGEFS) under research project A01L07UN070120180005, and the Algerian General Directorate for Scientific Research and Technological Development (DGRSDT), and the research laboratory (LI3CUB).

**Conflicts of Interest:** The author declares no conflict of interest.

## References

1. Dendouga, A.; Dendouga, A. High performance vector control of permanent magnet synchronous motor fed by direct SVM matrix converter. In Proceedings of the IEEE 4th International Conference on Power Electronics and Their Applications (ICPEA), Elazig, Turkey, 25–27 September 2019; pp. 1–6. [\[CrossRef\]](#)
2. Dendouga, A. A comparative study between the PI and SM controllers used by nonlinear control of induction motor fed by SVM matrix converter. *IETE J. Res.* **2020**, *1*–11. [\[CrossRef\]](#)
3. Pipolo, S.; Formentini, A.; Trentin, A.; Zanchetta, P.; Calvini, M.; Venturini, M. A New Modulation Approach for Matrix Converter. In Proceedings of the IEEE 2019 10th International Conference on Power Electronics and ECCE Asia (ICPE 2019—ECCE Asia), Busan, Korea, 27–30 May 2019; pp. 1021–1027.
4. Orcioni, S.; Biagetti, G.; Crippa, P.; Falaschetti, L. A Driving Technique for AC-AC Direct Matrix Converters Based on Sigma-Delta Modulation. *Energies* **2019**, *12*, 1103. [\[CrossRef\]](#)
5. Toledo, S.; Maqueda, E.; Rivera, M.; Gregor, R.; Wheeler, P.; Romero, C. Improved Predictive Control in Multi-Modular Matrix Converter for Six-Phase Generation Systems. *Energies* **2020**, *13*, 2660. [\[CrossRef\]](#)
6. Yao, P.; Jiang, X. An optimal six vector switching pattern in matrix converters for reducing harmonics and switching loss. *CSEE J. Power Energy Syst.* **2020**. [\[CrossRef\]](#)
7. Nguyen, H.-N.; Nguyen, M.-K.; Duong, T.-D.; Tran, T.-T.; Lim, Y.-C.; Choi, J.-H. A Study on Input Power Factor Compensation Capability of Matrix Converters. *Electronics* **2020**, *9*, 82. [\[CrossRef\]](#)
8. Nguyen, H.; Nguyen, T.D.; Lee, H. A modulation strategy to eliminate CMV for matrix converters with input power factor compensation. In Proceedings of the IECON 2016—42nd Annual Conference of the IEEE Industrial Electronics Society, Florence, Italy, 23–26 October 2016; pp. 6237–6242. [\[CrossRef\]](#)

9. Siwek, P. Input filter optimization for a DTC driven matrix converter-fed PMSM drive. In Proceedings of the 2018 IEEE 23rd International Conference on Methods & Models in Automation & Robotics (MMAR), Miedzyzdroje, Poland, 27–30 August 2018; pp. 35–40. [[CrossRef](#)]
10. Wang, X.; Lin, H.; Feng, B.; Lyu, Y. Damping of input LC filter resonance based on virtual resistor for matrix converter. In Proceedings of the IEEE Energy Conversion Congress and Exposition (ECCE), Raleigh, NC, USA, 15–20 September 2012; pp. 3910–3916. [[CrossRef](#)]
11. Deng, W.; Li, S. Direct torque control of matrix converter-fed PMSM drives using multi-dimensional switching table for common-mode voltage minimization. *IEEE Trans. Power Electron.* **2020**. [[CrossRef](#)]
12. Bounasla, N.; Hemsas, K.E. Second order sliding mode control of a permanent magnet synchronous motor. In Proceedings of the IEEE 14th International Conference on Sciences and Techniques of Automatic Control & Computer Engineering (STA), Sousse, Tunisia, 20–22 December 2013; pp. 535–539. [[CrossRef](#)]
13. Liu, J.; Zhang, Y. A universal maximum torque per ampere method for permanent magnet synchronous machines. In Proceedings of the IEEE 22nd International Conference on Electrical Machines and Systems (ICEMS), Harbin, China, 11–14 August 2019; pp. 1–5. [[CrossRef](#)]
14. Zhang, J.; Yang, H.; Wang, T.; Li, L.; Dorrell, D.G.; Lu, D.D. Field-oriented control based on hysteresis band current controller for a permanent magnet synchronous motor driven by a direct matrix converter. *IET Power Electron.* **2018**, *11*, 1277–1285. [[CrossRef](#)]
15. Yan, Y.; Zhao, J.; Xia, C.; Shi, T. Direct torque control of matrix converter-fed permanent magnet synchronous motor drives based on master and slave vectors. *IET Power Electron.* **2015**, *8*, 288–296. [[CrossRef](#)]
16. Peng, J.; Zhang, N.; He, L.; Shi, Q.; Lu, J. Sensorless vector control of permanent magnet synchronous motor based on DSP. In Proceedings of the IEEE 3rd Conference on Vehicle Control and Intelligence (CVCI), Hefei, China, 21–22 September 2019; pp. 1–4. [[CrossRef](#)]
17. Xiao, M.; Shi, T.; Yan, Y.; Xu, W.; Xia, C. Predictive torque control of permanent magnet synchronous motors using flux vector. *IEEE Trans. Ind. Appl.* **2018**, *54*, 4437–4446. [[CrossRef](#)]
18. Wang, T.; Liu, C.; Lei, G.; Guo, Y.; Zhu, J. Model predictive direct torque control of permanent magnet synchronous motors with extended set of voltage space vectors. *IET Electr. Power Appl.* **2017**, *11*, 1376–1382. [[CrossRef](#)]
19. Feng, Y.; Zhao, H.; Zhao, M.; Chen, H. A feedback linearization control scheme based on direct torque control for permanent magnet synchronous motor. In Proceedings of the 37th Chinese Control Conference (CCC), Wuhan, China, 25–27 July 2018; pp. 87–92. [[CrossRef](#)]
20. Fridman, L.; Levant, A. Higher order sliding modes. In *Book Sliding Mode Control in Engineering*; Barbot, J.P., Perruquett, W., Eds.; Marcel Dekker: New York, NY, USA, 2002; pp. 53–101. [[CrossRef](#)]
21. Borlaug, I.-L.G. Higher-Order Sliding Mode Control. Master’s Thesis, Norwegian University of Science and Technology, Trondheim, Norway, June 2017.
22. Utkin, V.; Poznyakb, A.; Orlov, Y.; Polyakov, A. Conventional and high order sliding mode control. *J. Frankl. Inst.* **2020**. [[CrossRef](#)]
23. Shtessel, Y.; Edwards, C.; Fridman, L.; Levant, A. *Sliding Mode Control and Observation*; Springer: New York, NY, USA, 2014; pp. 1–356. [[CrossRef](#)]
24. Gu, P.; Wang, X.; Reitz, M. High order sliding mode control of permanent magnet synchronous generator-based wind energy conversion systems. In Proceedings of the IEEE Energy Conversion Congress and Exposition (ECCE), Milwaukee, WI, USA, 18–22 September 2016; pp. 1–8. [[CrossRef](#)]
25. Levant, A. Robust exact differentiation via sliding mode technique. *Automatica* **1998**, *34*, 379–384. [[CrossRef](#)]

